Submitted to Optics Communications (August 2003) 2690

Laser operation of a low loss (0.1 dB/cm) Nd:$Gd_3Ga_5O_{12}$ thick (40 μm) planar waveguide grown by pulsed laser deposition

C. Grivas (*), T.C. May-Smith, D.P. Shepherd, R.W. Eason

Optoelectronics Research Centre (O.R.C.), University of Southampton,

Highfield, Southampton SO17 1BJ, United Kingdom

PACS: 42.70.Hj; 42.55.-f, 42.82.Et, 42.79.Gn; 78.20; 81.15.Fg

Keywords: laser materials, lasers, waveguides, optical waveguides, laser deposition

* Corresponding author.

E-mail: chg@orc.soton ac.uk, Tel.: ++44 (0)2380 593141, Fax: ++44 (0) 2380 593142

Abstract

Waveguiding films of Nd:$Gd_3Ga_5O_{12}$ with a thickness up to 40 μm have been fabricated by pulsed-laser deposition on $Y_3Al_5O_{12}$ (100) substrates. A laser threshold of 18 mW of absorbed pump power has been obtained and lasing action has been observed at 1060.6 nm for pump powers close to the lasing threshold, and at both 1059.0 and 1060.6 nm at pump power levels of approximately 1.5 times above threshold. Waveguide propagation losses of 0.1dB/cm have been obtained by measuring the absorbed pump power threshold for laser operation at 1060.6 nm for a range of output couplers with various reflectivities. Slope efficiencies of 12.3% and 17.5% were derived using output couplers with a transmission of 2.2% and 4.5% respectively. The combination of low propagation losses and high numerical aperture for the waveguides indicates the potential of the fabrication technique to produce high quality thick multi-layer waveguides. Such designs are suitable for the development of high-power diode-pumped laser sources of near-diffraction-limited beam quality.

1. Introduction

Planar waveguide lasers have attracted increased attention in the last years particularly with a view to developing high average power diode-pumped solid state lasers for a broad spectrum of applications. For diode-pumped schemes, the planar waveguide design can address four general requirements for optimal laser performance: (a) efficient coupling of the diode bar pump light into the guide due to both the excellent geometric match of the pump beam to the profile of waveguide facet as well as the possibility to confine non diffraction limited beams by designing high numerical aperture structures, (b) control of the spatial output of the waveguide by introducing design schemes such as double-cladding [1], large-mode-area waveguides [2], multimode interference [3] as well as tapers [4] and unstable resonators [5], (c) possibility of efficient thermal handling and therefore, circumvention of problems such as thermal lensing, birefringence and fracture [6] and (d) in combination with the selection of a suitable fabrication technique, development of structures with low propagation losses.

In an attempt to develop thick waveguiding layers as laser sources, which would combine characteristics such as high numerical apertures (NA) together with low propagation loss, we report here an investigation of the lasing and waveguiding characteristics of planar Nd:$Gd_3Ga_5O_{12}$ (Nd:GGG) thick films fabricated by pulsed laser deposition (PLD). The motivation for thick film growth is the subsequent development of multilayered waveguides with a thickness of several tens of microns as the planar analogues of the large-mode-area (LMA) and cladding-pumped LMA waveguide designs previously used in optical fibres [7, 8]. This would enable us to produce high-power diode-pumped laser sources of near-diffraction-limited beam quality at output powers in the order of tens or possibly up to one hundred Watts. PLD has been proven a reliable technique for the growth of waveguiding films of various laser host materials. Lasing has so far been observed in PLD grown Nd:GGG

[9, 10] and Ti:sapphire planar guides [11]. One of the advantages offered by this fabrication method is the potential to produce high NA waveguides, which in the case of the Nd:GGG (refractive index 1.97) growth on YAG (refractive index 1.82) substrates is 0.75.

This paper reports PLD growth of high-quality thick (up to 40 μm) Nd:GGG layers with very low propagation loss (~0.1 dB/cm), which is a significant improvement over the performance of previously reported structures (~0.5 dB/cm) [12]. Additionally, we have demonstrated laser operation of these films and investigated their performance in terms of absorbed pump power threshold and output slope efficiencies. Finally, to evaluate the device performance, calculations of the expected output accounting for the propagation loss were carried out and we show that the theoretical and experimental values are in good agreement.

2. Waveguide fabrication and laser performance

Depositions were performed in a stainless steel vacuum chamber, which was evacuated down to a base pressure of $5x10^{-6}$ mbar. Films were grown by pulsed laser ablation of a single crystal Nd:$Gd_3Ga_5O_{12}$ target of 1-at% concentration in Nd^{3+} in a background oxygen atmosphere of $2x10^{-2}$ mbar. Ablation was provided by a KrF excimer laser (Lambda Physik, LPX 200, 248 nm, pulse duration ~20 ns) operated at 10 Hz, and focused to an energy density of ~2 J/cm^2 on the target. Films were deposited on single crystal $Y_3Al_5O_{12}$ (100) substrates positioned at a distance of 4 cm away from the target material. All films used for the investigation were grown at a substrate temperature of ~650°C and had a thickness up to ~40 μm. To localize the substrate heating and to prevent contamination through desorption from the walls of the deposition chamber, a 50 W CO_2 laser (Synrad 57-1-28W) was used as a heating source, a technique that has already been implemented successfully in PLD [13, 14]. The growth of thick Nd:GGG layers together with their morphological, compositional and structural properties has been detailed elsewhere [15].

********** FIGURE 1 **********

To investigate the fluorescence characteristics of the waveguide the sample was cut to a length of 4.1 cm and its faces were subsequently polished to an optically smooth finish. The fluorescence emission from the Nd:GGG layer was obtained by coupling the 808 nm irradiation from a Ti:sapphire laser (Spectra Physics, Model 3900S) into the waveguide and observing the output with a spectrum analyzer (Hewlett Packard 86140A). Figure 1 shows fluorescence spectra around the 1060 nm region, which correspond to the transition, $^4F_{3/2} \rightarrow {}^4I_{11/2}$, for both the bulk crystal target and the PLD grown waveguide. The spectra are plotted normalized to the same total area under all the fluorescence lines. The broadening and shift in the spectrum from the waveguide in comparison with that of the bulk material is likely to be due to the stress induced by the lattice mismatch of the epitaxially grown waveguide film with respect to the YAG substrate, as well as a slight gallium deficiency in the PLD film.

********** FIGURE 2 **********

For the investigation of the laser performance of the Nd:GGG waveguide the output from the Ti:sapphire laser operating at 808 nm was launched into the waveguide by a spherical lens with a focal length of 5 cm so that the beam was focused to a spot diameter of ~11 μm at the input face of the sample. Guided light from the waveguide was coupled out with a microscope objective with a magnification of x10 and was subsequently detected by a photodiode and displayed on an oscilloscope. The laser cavity was formed by attaching lightweight thin mirrors at the end faces of the sample using the surface tension of a small amount of fluorinated liquid. In this configuration the input mirror of the Fabry-Perot cavity had a reflectivity R_1 of 99.8% and a transmission of 94% at the lasing and pump wavelength respectively. A set of five mirrors with varying transmission values T_2 of 0.2% (HR mirror), 1.8%, 2.2%, 4.5%, and 12% at the laser wavelength, were successively used as output couplers and the lasing threshold was measured for each of them. A threshold of 18 mW was obtained when a high reflectivity mirror (T_2 = 0.2%) was used as an output coupler. For absorbed pump powers close to the threshold, lasing occurred at 1060.6 nm, corresponding to

the most intense peak of the fluorescence spectrum, while for absorbed powers above 60 mW simultaneous lasing at 1059.0 and 1060.6 nm was observed. Figures 2a and 2b show typical lasing spectra obtained at 35 mW, which is the threshold for the appearance of the second band and at 100 mW, where both bands are present, respectively. Due to the insufficient resolution of the spectrum analyzer no individual longitudinal modes can be observed. However, from the separation of the ripples that can be seen on the top of the two emission bands we can infer that these ripples correspond to the longitudinal cavity modes calculated from the 4.1 mm cavity length. By successively replacing the HR output coupling mirror (T_2 = 0.2%) with two mirrors with T_2 = 2.2% and 4.5%, the threshold value increased from 18 mW to 36 and 54 mW respectively. Figure 3 shows the output power as a function of the absorbed pump power using the T_2 = 2.2% and 4.5% output couplers with slope efficiencies of 12.3% and 17.5% respectively. The absorbed pump power was calculated from the incident power by measuring the product (LxA) of the launch efficiency, L, and the single-pass absorption, A. This was achieved by comparison of the total transmitted pump power obtained when launching the pump beam into the guide with that transmitted when the pump is focused directly through the substrate [16].

********** FIGURE 3 **********

Observation of the laser mode has been performed by imaging the emission from the waveguide on a CCD camera. Figure 4 shows the output laser beam obtained with an output coupler of T_2 = 2.2% for an absorbed pump power of 55 mW, which is approximately 1.5 times the threshold value. It can be seen that the beam was multimode with 3 lobes in the plane perpendicular to the waveguide and had a diameter of ~40 μm, which is the same size as the waveguide thickness. In the other plane the output beam had a diameter of ~100 μm and measurement of its profile suggests that it was multimode in this direction too.

********** FIGURE 4 **********

The investigation of the laser performance of the Nd:GGG waveguide also allowed an evaluation of the propagation loss via the Findley-Clay method [17]. For a four-level-laser

system with negligible depopulation of the ground state the absorbed power threshold P_{th}, is dependent on the level of the output coupling and the propagation attenuation coefficient and can be expressed as:

$$P_{th} = K \cdot [(2 \cdot \alpha_L \cdot l - \ln(R_1 R_2)] \quad (1)$$

where l is the length of the waveguide, R_1 and R_2 are the intensity reflectivities of the in- and out-coupling mirrors respectively, α_L is the propagation attenuation coefficient and K is a constant given by [18]:

$$K = \frac{\pi \cdot h \cdot \nu_p}{4 \cdot \tau \cdot \sigma_e} \cdot \sqrt{w_{lx}^2 + w_{px}^2} \cdot \sqrt{w_{ly}^2 + w_{py}^2} \quad (2)$$

where h is Planck's constant, ν_p is the frequency of the pump irradiation, τ = 160 μs is the excited state lifetime as measured in [5] for waveguides and the bulk crystal (τ = 180 μs) [19] with the same concentrations of Nd^{3+} as the films studied in this work, w_{lx}, w_{ly}, w_{px}, w_{py}, are the average $1/e^2$ radii of intensity of the laser and pump modes in the horizontal and vertical directions respectively, and σ_e (=7.7x10^{-24} m^2) is the emission cross section. We note that this value for the emission cross section has been derived by multiplying the value given in [20] (σ_e = 2.1x10^{-23} m^2) for the bulk material by a factor of 0.365. This correction factor was obtained by plotting the fluorescence spectra of the waveguide and the bulk target such that the same total area is contained under all the fluorescence lines, as shown in Fig. 1b and then comparing the corresponding peak heights.

A plot of P_{th}/l against $-\ln(R_1 R_2)/2 \cdot l$ for the set of different output coupling mirrors used in our experiment is shown in Figure 5. Such an analysis allows estimation of the propagation attenuation coefficient α_L from the intercept on the x-axis, which in this case gives a value of $\alpha_L \sim 2$ m^{-1}. A propagation loss in the active layer of 0.1 dB/cm can then be calculated, which to the best of our knowledge is the lowest loss ever reported for any PLD grown waveguide. Apart from the propagation in the waveguide the above loss value may

also account for any possible losses originating from the non-uniformity of the mirror attachment over the length of the waveguide faces as well as from misalignment of the cavity itself, resulting from the non-perfectly parallel end faces of the waveguide.

********** FIGURE 5 **********

3. Slope efficiency and laser threshold considerations

We now estimate the slope efficiencies expected from the lasing waveguide following an analysis that incorporates effects of transverse mode profiles on the slope efficiency in longitudinally pumped lasers [21]. Assuming that both the pump and laser beam have Gaussian (TEM_{00}) profiles then according to the proposed model the slope efficiency is given by:

$$\eta = \eta_q \frac{\nu_l}{\nu_p} \cdot \frac{-\ln(R_2)}{-\ln(R_1 \cdot R_2) + (2 \cdot \alpha_L \cdot l)} \cdot \eta_{pl} \tag{3}$$

where R_1 and R_2 are the intensity reflectivities of the input and output couplers respectively, η_q represents the quantum efficiency of the device (assumed to be 100%, so that for every pump photon one laser photon is produced), ν_p and ν_l are the frequencies of the pump and the laser radiation respectively, α_L is the propagation attenuation coefficient, and η_{pl} is a parameter that contains the overlap and geometrical factors associated with the conversion of pump photons into laser emission and is given by the expression:

$$\eta_{pl} = \frac{w_{lx} \cdot w_{ly} \cdot (2w_{px}^2 + w_{lx}^2)^{1/2} \cdot (2w_{py}^2 + w_{ly}^2)^{1/2}}{(w_{px}^2 + w_{lx}^2) \cdot (w_{py}^2 + w_{ly}^2)} \tag{4}$$

where w_{lx} , w_{ly}, w_{px}, w_{py} as mentioned previously are the $1/e^2$ intensity radii of the laser and pump modes in the horizontal and vertical directions respectively. As an approximation for the 100 μm x 40 μm waveguide laser beam (as measured using the CCD camera) we assume single mode profiles with $1/e^2$ intensity radii of w_{lx} = 33.3 μm and w_{ly}= 13.3 μm for the x and y axes respectively. This assumption will enable a prediction of the maximum expected values for the slope efficiencies. For the pump beam, whose waist during the lasing

experiments was located with a good accuracy at the input face of the sample, we assume a mode size ($1/e^2$ intensity) of w_{px}=3.6 μm and w_{py}=13.3 μm for the unguided and guided direction respectively. This value for the guided direction has been derived by assuming a pump beam diameter of 40 μm, which is equal to the thickness of the guide. As for the unguided direction, for a fundamental Gaussian beam such as the pump beam, its size at any location within the waveguide can be obtained by the expression [22]:

$$w_p^2(z) = w_p^2\left[1+\left(\frac{\lambda_p\cdot(z-z_p)}{\pi\cdot w_p^2\cdot n}\right)^2\right] \tag{5}$$

where λ_p is the pump wavelength, n is the refractive index of the waveguide, and z_p stands for the location of the pump waist inside the waveguide and is set as zero since we assume focusing of the pump beam at the input face of the waveguide. The average value $\overline{w_p}$ of the pump beam radius along the waveguide is then expressed by [22]:

$$\overline{w_p^2} = \frac{1}{l}\cdot\int_0^l w_p^2(z)\cdot dz \tag{6}$$

From (5) and (6) we calculate an average modal radius of w_{lx}=86 μm while for w_{ly} we assume a value of 13.3 μm. By inserting the modal dimensions for the pump and laser beam in (2) and from equation (1) we obtain for output coupling mirrors with T_2 = 2.2% and 4.5% slope efficiencies of 17.6% and 23.1% respectively. Despite the approximate nature of this calculation these values are in broad agreement with the experimentally obtained ones, which were 12.3% and 17.5% respectively, thus illustrating consistency of the output levels with a structure characterized by an internal propagation loss of 0.1 dB/cm. The discrepancy is attributed to the fact that in our calculation of the overlap of the pump and laser mode we have not taken into account the multimode nature of the laser beam. The bad overlap would yield lower values for the parameter η_{pl} which in turn over-estimates the calculated efficiencies.

To make a prediction of lasing threshold for the 40 μm thick waveguide we calculate

the parameter K from equation (1). From equation (2) and using HR mirrors ($R_1 = R_2 =$ 99.8%) as input and output couplers we obtain a value of 5.7 mW for the absorbed power threshold, which is ~3 times less than the experimentally obtained one (18 mW). This difference is likely to be due to an inaccuracy of the figure assumed for the emission cross section for the bulk target material.

4. Conclusions

In summary, thick Nd:GGG films have been grown by pulsed laser deposition on undoped YAG substrates. Laser action has been demonstrated at 1059.0 and 1060.6 nm and propagation losses as low as 0.1 dB/cm, which we believe to be the lowest levels ever recorded in laser fabricated waveguides, have been obtained by investigating the dependence of the absorbed power threshold on the output coupling level. The threshold value for lasing at 1060.6 was 18 mW with a slope efficiency of 17.5% with respect to the absorbed power using an output coupler with a transmission of 4.5%. Furthermore, calculations of the slope efficiency and lasing threshold have provided values that are in broad agreement with the experimentally obtained ones. Slope efficiency levels could increase by improving the overlap of the pump and laser modes however, at this point our main interest was assessment of the overall performance of such thick films to determine prior art for more sophisticated multilayer waveguide designs. Further work is in progress towards the development of multi-layer garnet waveguides, for which such thickness is essential, as the planar analogues of the LMA and cladding-pumped LMA waveguide designs suitable for high-power diode-pumping and capable of delivering high output powers (10-100 W) of near-diffraction-limited beam quality.

Acknowledgements

This research was supported by the Engineering and Physical Sciences Research Council

(EPSRC) under the grant GR/R74154/01. One of the authors (T.C.M-S) wishes to acknowledge the EPSRC for a studentship.

Figure Captions

Figure 1. Fluorescence spectra of the Nd:GGG planar waveguide (full line) and the bulk crystal target (dash-dotted line) for the $^4F_{3/2} \rightarrow {}^4I_{11/2}$ transition in the 1060 nm spectral region.

Figure 2. Typical lasing spectra of the Nd:GGG waveguide for absorbed pump powers of (a) 35 mW and (b) 100 mW. The ripples shown in the emission band correspond to longitudinal cavity modes.

Figure 3. Dependence of the output power as a function of the absorbed power for two output couplers: (□) 2.2% and (●) 4.5% transmission respectively.

Figure 4. Laser mode profile obtained from the Nd:GGG waveguide using a 2.2% output coupler at an absorbed power of 55 mW.

Figure 5. A plot of P_{th}/l as a function of $-\ln(R_1 R_2)/2 \cdot l$. The position of the intercept on the x axis yields the propagation attenuation coefficient (α_L~2 m^{-1}).

References

[1] C.L. Bonner, T. Bhutta, D.P. Shepherd, A. Tropper, IEEE J. Quant. Elect. 36 (2000) 236.

[2] H.L. Offerhaus, N.G. Broderick, D.J. Richardson, R. Sammut, J. Caplen, L. Dong, Opt. Lett. 23 (2000) 1683.

[3] H.J. Baker, J.R. Lee, D.R.Hall, Opt. Express 10 (2002) 297

[4] S.J. Hettrick, J.I. MacKenzie, R.D. Harris, J.S. Wilkinson, D.P. Shepherd, A. Tropper, Opt. Lett. 25 (2000) 1433.

[5] R.J. Beach, S.C. Mitchell, H.E. Meissner, O.R. Meissner, W.F. Krupke, J.M. McMahon, W.J. Bennett, D.P. Shepherd, Opt. Lett. 26 (2001) 881.

[6] D.P. Shepherd, S.J. Hettrick, J.I. MacKenzie, C. Li, R.J. Beach, S.C. Mitchell, H.E. Meissner, J. Phys. D: Appl. Phys. 34 (2001) 2420.

[7] H.L. Offerhaus, N.G. Broderick, D.J. Richardson, R. Sammut, J. Caplen, and L. Dong, Opt. Lett. 23 (1998) 1683.

[8] E. Snitzer, H. Po, F. Hakimi, R. Tumminelli, B.C. McCollum, Proc. of Conference on Optical Fiber Communication, 1988, paper PD5.

[9] D.S. Gill, A.A. Anderson, R.W. Eason, T.J. Warburton, D.P. Shepherd, Appl. Phys. Lett. 69 (1996) 10.

[10] C.L. Bonner, A.A. Anderson, R.W. Eason, D.P. Shepherd, D.S. Gill, C. Grivas, N.A. Vainos, Opt. Lett. 22 (1997) 988.

[11] A.A. Anderson, R.W. Eason, L.M.B. Hickey, M. Jelinek, C. Grivas, D.S. Gill, N.A. Vainos, Opt. Lett. 22 (1997) 1556.

[12] A.A. Anderson, C.L. Bonner, D.P. Shepherd, R.W. Eason, C. Grivas, D.S. Gill, N.A. Vainos, Opt. Commun. 144 (1997) 183.

[13] A.A. Anderson, R.W. Eason, M. Jelinek, C. Grivas, D. Lane K. Rodgers, L.M.B. Hickey, C. Fotakis, Thin Solid Films 300 (1997) 68.

[14] S.J. Barrington, R.W. Eason, Rev. Sci. Instrum., 71 (2000) 4223.

[15] T.C. May-Smith, C. Grivas, D.P. Shepherd, R.W. Eason, Appl. Surf. Sci. (submitted for publication)

[16] D. Pelenc, B. Chambaz, I. Chartier, B. Ferrand, C. Wyon, D.P. Shepherd, D.C. Hanna, A.C. Large, A.C. Tropper, Opt. Commun. 115 (1995) 491.

[17] D. Findley, R.A. Clay, Phys. Lett. 20 (1966) 277.

[18] W.P. Risk, J. Opt. Soc. Am. B 5 (1988) 1412.

[19] S.J. Field, D.C. Hanna, A.C. Large, D.P. Shepherd, A.C. Tropper, P.J. Chandler, P.D. Townsend, L. Zhang, Opt. Commun. 86 (1991) 161.

[20] M.D. Rotter, B. Dane, Opt. Commun. 198 (2001) 155.

[21] W.A. Clarkson, D.C. Hanna, J. Mod. Opt. 36 (1985) 483.

[22] M.J.F. Digonnet, C.J. Gaeta, Appl. Opt. 24 (1985) 333.

FIGURE 1 : C. Grivas et al. "Laser operation of ...laser deposition"

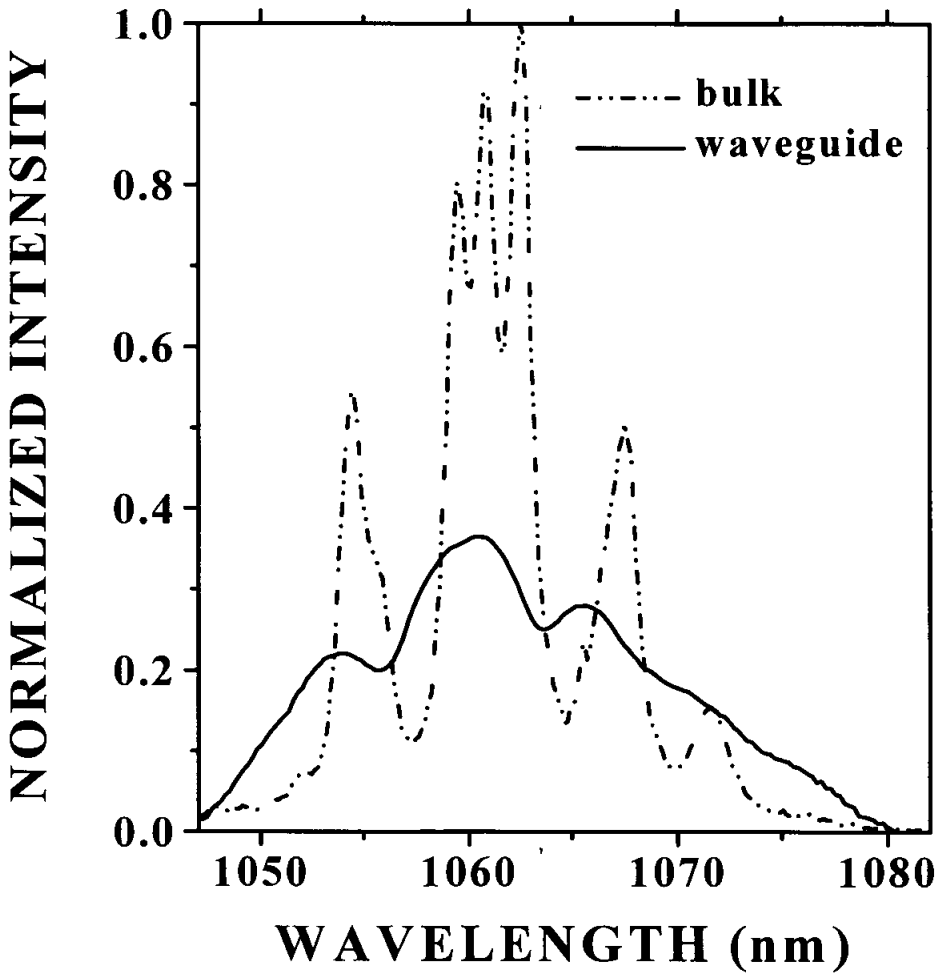

FIGURE 2 : C. Grivas et al. "Laser operation of ...laser deposition"

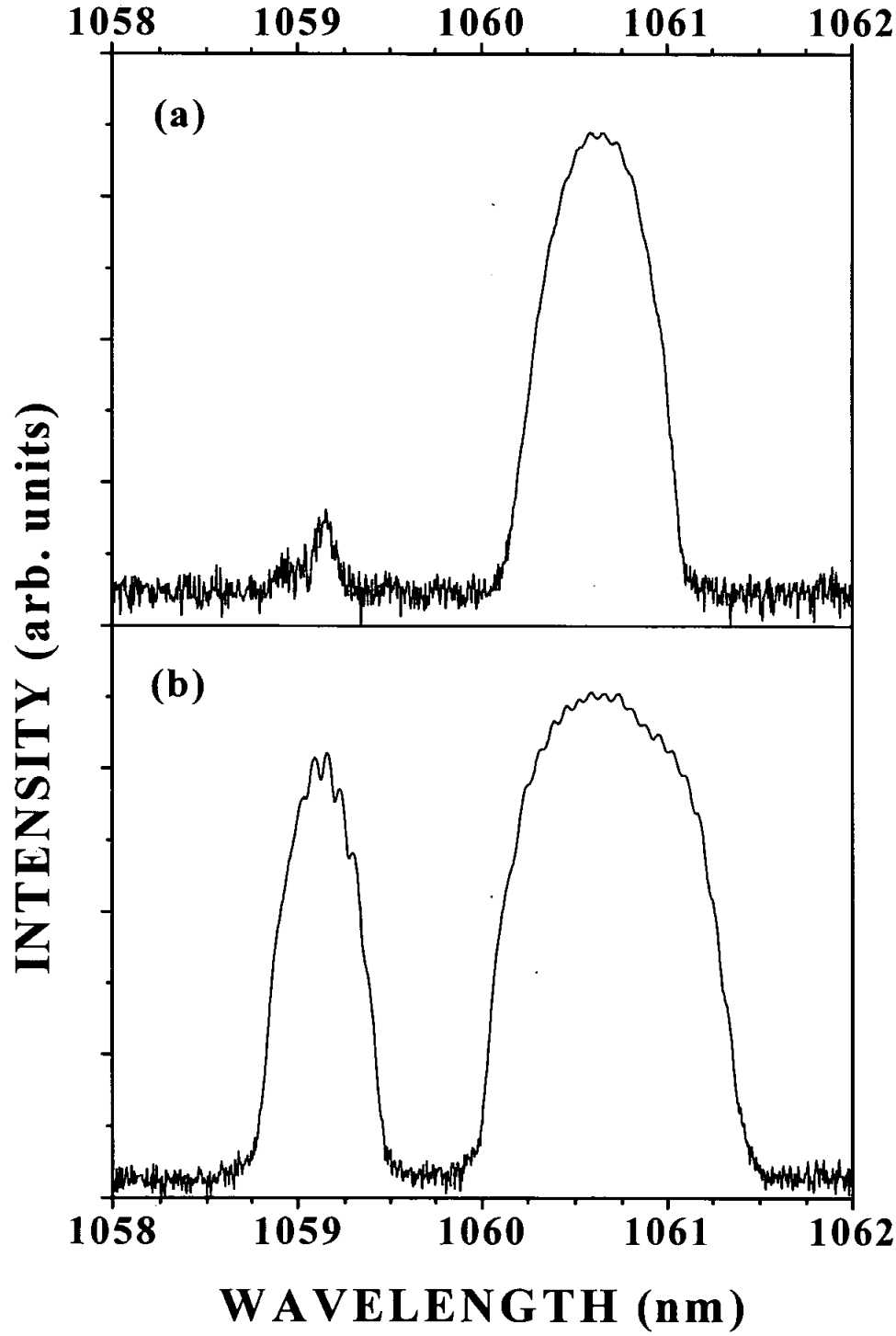

FIGURE 3 : C. Grivas et al. "Laser operation of ...laser deposition"

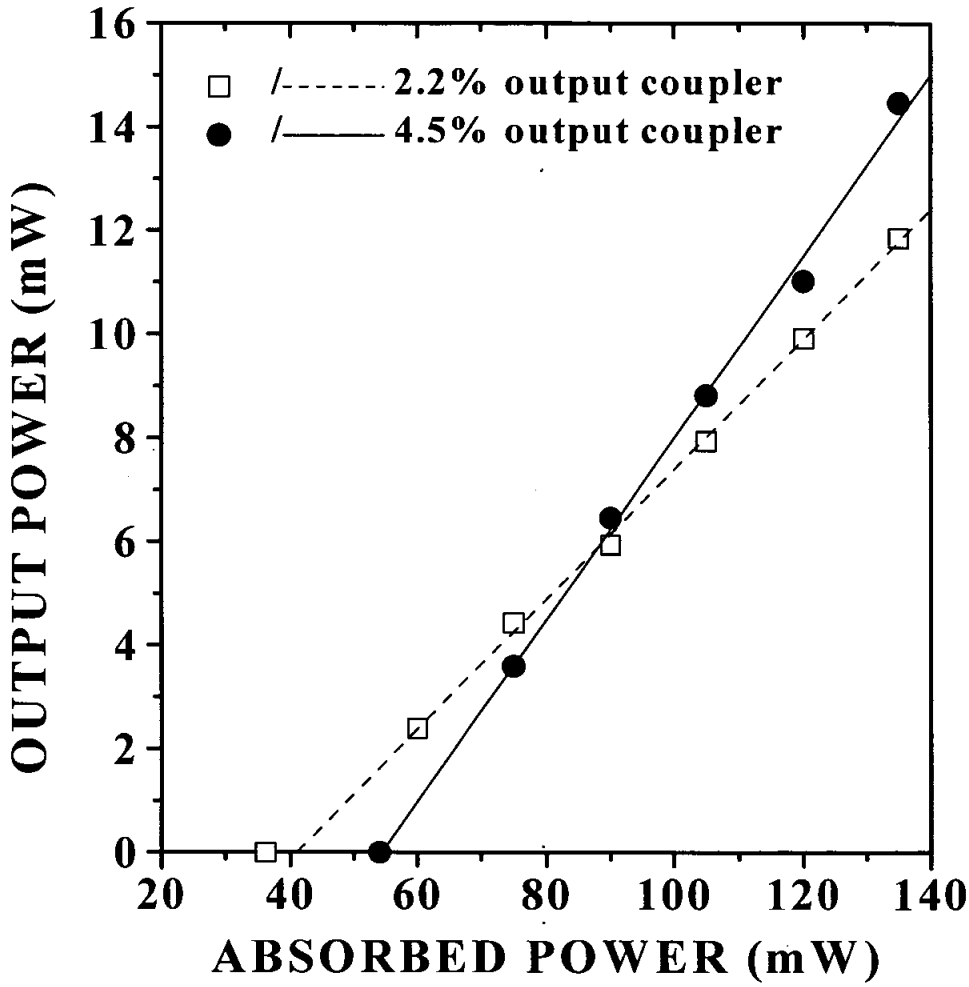

FIGURE 4 : C. Grivas et al. "Laser operation of ...laser deposition"

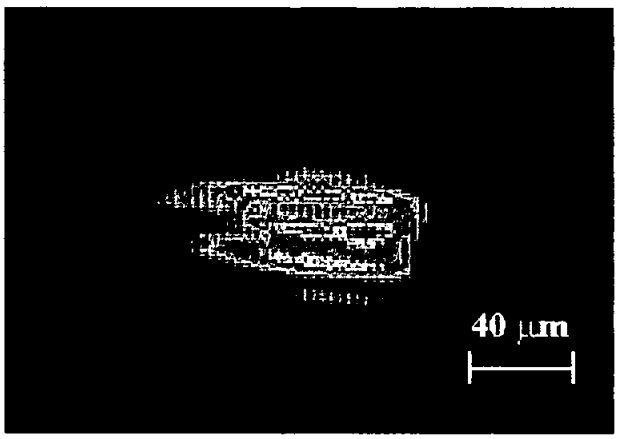

FIGURE 5 : C. Grivas et al. "Laser operation of ...laser deposition"